

InGaAs PIN photodetectors integrated on silicon-on-insulator waveguides

Zhen Sheng,^{1,2,*} Liu Liu,^{1,3} Joost Brouckaert,¹ Sailing He,² and Dries Van Thourhout¹

¹ INTEC Department, Photonics Research Group, Ghent University-IMEC, St-Pietersnieuwstraat 41, 9000 Gent, Belgium

² Centre for Optical and Electromagnetic Research, State Key Laboratory for Modern Optical Instrumentation, Zhejiang University, Zijingang Campus, Hangzhou 310058, China

³ Currently with Department of Photonics Engineering, Technical University of Denmark, DTU - Fotonik, DK-2800 Kongens Lyngby, Denmark

*sheng.zhen@intec.ugent.be

Abstract: InGaAs PIN photodetectors heterogeneously integrated on silicon-on-insulator waveguides are fabricated and characterized. Efficient evanescent coupling between silicon-on-insulator waveguides and InGaAs photodetectors is achieved. The fabricated photodetectors can work well without external bias and have a very low dark current of 10pA. The measured responsivity of a 40 μ m-long photodetector is 1.1A/W (excluding the coupling loss between the fiber and the SOI waveguide) at a wavelength of 1550nm and shows good linearity for an input power range of 40dB. Due to the large absorption coefficient of InGaAs and the efficient evanescent coupling, the fabricated photodetectors can cover the whole S, C and L communication bands.

©2010 Optical Society of America

OCIS codes: (040.5160) Photodetectors; (250.3140) Integrated optoelectronic circuits.

References and links

1. R. Soref, and J. Lorenzo, "All-silicon active and passive guided-wave components for $\lambda = 1.3$ and $1.6 \mu\text{m}$," IEEE J. Quantum Electron. **22**(6), 873–879 (1986).
2. R. Soref, and B. Bennett, "Electrooptical effects in silicon," IEEE J. Quantum Electron. **23**(1), 123–129 (1987).
3. W. Bogaerts, D. Taillaert, B. Luyssaert, P. Dumon, J. Van Campenhout, P. Bienstman, D. Van Thourhout, R. Baets, V. Wiaux, and S. Beckx, "Basic structures for photonic integrated circuits in Silicon-on-insulator," Opt. Express **12**(8), 1583–1591 (2004).
4. T. Tsuchizawa, K. Yamada, H. Fukuda, T. Watanabe, J. Takahashi, M. Takahashi, T. Shoji, E. Tamechika, S. Itabashi, and H. Morita, "Microphotonics devices based on silicon microfabrication technology," IEEE J. Sel. Top. Quantum Electron. **11**(1), 232–240 (2005).
5. H. Rong, A. Liu, R. Jones, O. Cohen, D. Hak, R. Nicolaescu, A. Fang, and M. Paniccia, "An all-silicon Raman laser," Nature **433**(7023), 292–294 (2005).
6. A. W. Fang, H. Park, O. Cohen, R. Jones, M. J. Paniccia, and J. E. Bowers, "Electrically pumped hybrid AlGaInAs-silicon evanescent laser," Opt. Express **14**(20), 9203–9210 (2006).
7. G. Roelkens, D. Van Thourhout, R. Baets, R. Nötzel, and M. Smit, "Laser emission and photodetection in an InP/InGaAsP layer integrated on and coupled to a Silicon-on-Insulator waveguide circuit," Opt. Express **14**(18), 8154–8159 (2006).
8. A. Liu, R. Jones, L. Liao, D. Samara-Rubio, D. Rubin, O. Cohen, R. Nicolaescu, and M. Paniccia, "A high-speed silicon optical modulator based on a metal-oxide-semiconductor capacitor," Nature **427**(6975), 615–618 (2004).
9. Q. Xu, B. Schmidt, S. Pradhan, and M. Lipson, "Micrometre-scale silicon electro-optic modulator," Nature **435**(7040), 325–327 (2005).
10. J. Liu, J. Michel, W. Giziewicz, D. Pan, K. Wada, D. D. Cannon, S. Jongthammanurak, D. T. Danielson, L. C. Kimerling, J. Chen, F. Ö. Ilday, F. X. Kärtner, and J. Yasaitis, "High-performance, tensile-strained Ge p-i-n photodetectors on a Si platform," Appl. Phys. Lett. **87**(10), 103501 (2005).
11. G. Roelkens, J. Brouckaert, D. Taillaert, P. Dumon, W. Bogaerts, D. Van Thourhout, R. Baets, R. Nötzel, and M. Smit, "Integration of InP/InGaAsP photodetectors onto silicon-on-insulator waveguide circuits," Opt. Express **13**(25), 10102–10108 (2005).
12. G. Roelkens, D. Van Thourhout, R. Baets, R. Nötzel, and M. Smit, "Laser emission and photodetection in an InP/InGaAsP layer integrated on and coupled to a Silicon-on-Insulator waveguide circuit," Opt. Express **14**(18), 8154–8159 (2006).
13. M. Kostrzewa, L. Di Cioccio, M. Zussy, J. C. Roussin, J. M. Fedeli, N. Kernevez, P. Regreny, C. Lagahe-Blanchard, and B. Aspar, "InP dies transferred onto silicon substrate for optical interconnects application," Sens. Actuators A Phys. **125**(2), 411–414 (2006).

14. T. Maruyama, T. Okumura, and S. Arai, "Direct wafer bonding of GaInAsP/InP membrane structure on silicon-on-insulator substrate," *Jpn. J. Appl. Phys.* **45**(11), 8717–8718 (2006).
15. G. Roelkens, J. Brouckaert, D. Van Thourhout, R. Baets, R. Nötzel, and M. Smit, "Adhesive Bonding of InP/InGaAsP Dies to Processed Silicon-On-Insulator Wafers using DVS-bis-Benzocyclobutene," *J. Electrochem. Soc.* **153**(12), G1015–G1019 (2006).
16. I. Christiaens, G. Roelkens, K. De Mesel, D. Van Thourhout, and R. Baets, "Thin-film devices fabricated with benzocyclobutene adhesive wafer bonding," *J. Lightwave Technol.* **23**(2), 517–523 (2005).
17. A. Jourdain, P. De Moor, K. Baert, I. De Wolf, and H. A. C. Tilmans, "Mechanical and electrical characterization of BCB as a bond and seal material for cavities housing (RF-) MEMS devices," *J. Micromech. Microeng.* **15**(7), S89–96 (2005).
18. M. Jutzi, M. Berroth, G. Wöhl, M. Oehme, and E. Kasper, "Ge-on-Si vertical incidence photodiodes with 39-GHz bandwidth," *IEEE Photon. Technol. Lett.* **17**(7), 1510–1512 (2005).
19. L. Chen, P. Dong, and M. Lipson, "High performance germanium photodetectors integrated on submicron silicon waveguides by low temperature wafer bonding," *Opt. Express* **16**(15), 11513–11518 (2008).
20. L. Chen, and M. Lipson, "Ultra-low capacitance and high speed germanium photodetectors on silicon," *Opt. Express* **17**(10), 7901–7906 (2009).
21. L. Vivien, J. Osmond, J. M. Fédéli, D. Marris-Morini, P. Crozat, J. F. Damlencourt, E. Cassan, Y. Lecunff, and S. Laval, "42 GHz p-i-n Germanium photodetector integrated in a silicon-on-insulator waveguide," *Opt. Express* **17**(8), 6252–6257 (2009).
22. D. Taillaert, F. Van Laere, M. Ayre, W. Bogaerts, D. Van Thourhout, P. Bienstman, and R. Baets, "Grating couplers for coupling between optical fibers and nanophotonic waveguides," *Jpn. J. Appl. Phys.* **45** (No. 8A), 6071–6077 (2006).
23. J. Bowers, and C. A. Burrus, "Ultrawide-band long-wavelength p-i-n photodetectors," *J. Lightwave Technol.* **5**(10), 1339–1350 (1987).
24. M. R. Amersfoort, M. K. Smit, Y. S. Oei, I. Moerman, and P. Demeester, "Simple method for predicting absorption resonances of evanescently-coupled waveguide photodetectors," in *Proceedings of 6th European Conference on Integrated Optics*, (Neuchitel, Switzerland, 1993), pp. 2–40–2–41.
25. Z. Sheng, L. Liu, J. Brouckaert, S. He, D. Van Thourhout, and R. Baets, "Investigation of evanescent coupling between SOI waveguides and heterogeneously-integrated III-V pin photodetectors," in *Proceedings of 21st IEEE International Conference on Indium Phosphide & Related Materials*, (IEEE, Newport Beach, CA, 2009), pp. 159–162.
26. H. Park, A. W. Fang, R. Jones, O. Cohen, O. Raday, M. N. Sysak, M. J. Paniccia, and J. E. Bowers, "A hybrid AlGaInAs-silicon evanescent waveguide photodetector," *Opt. Express* **15**(10), 6044–6052 (2007).
27. J. Brouckaert, G. Roelkens, D. Van Thourhout, and R. Baets, "Compact InAlAs–InGaAs metal–semiconductor–metal photodetectors integrated on silicon-on-insulator waveguides," *IEEE Photon. Technol. Lett.* **19**(19), 1484–1486 (2007).
28. W. Bogaerts, P. Dumon, D. Van Thourhout, D. Taillaert, P. Jaenen, J. Wouters, S. Beckx, V. Wiaux, and R. Baets, "Compact wavelength-selective functions in silicon-on-insulator photonic wires," *IEEE J. Sel. Top. Quantum Electron.* **12**(6), 1394–1401 (2006).

1. Introduction

Silicon photonics, although proposed over twenty years ago [1,2], is still attracting a growing research interest in recent years. The main motivation is its fabrication process which is compatible with the complementary-metal-oxide-semiconductor (CMOS) electronics industry. One of the current research trends in silicon photonics is to integrate many kinds of optical functionalities on a single chip, including passive and active devices. Tremendous work [3–12] has been done towards this aim. Although silicon is widely recognized as an excellent material for light guiding beyond the wavelength of 1.1 μm , it is outperformed by III–V semiconductor materials for active functions, such as light generation and detection at telecom wavelengths (1.31–1.55 μm), due to its intrinsic material limitations. These III–V materials can be heterogeneously integrated on silicon platform by means of a wafer bonding process [6,13–15]. We have developed a low-temperature die-to-wafer bonding process with divinylsiloxane benzocyclobutene (DVS-BCB) as the bonding layer [15]. The fabrication process consists of bonding unprocessed III-V dies (epitaxial layers down) onto a processed SOI substrate, removal of the III-V substrate, and subsequent wafer-scale processing for the III-V devices with lithographical alignment accuracy to the underlying SOI structures. Various active components, such as lasers [7] and photodetectors [11], have been demonstrated based on this platform. The BCB bonding has also been proved good reliability in both photonic [16] and MEMs applications [17].

Photodetectors are one of the most important devices for photonic integrated circuits, and convert optical signals into the electrical form. Germanium photodetectors integrated on SOI have been demonstrated for the wavelength range of 1.3 μm and 1.5 μm and have the

advantage of complete compatibility with CMOS processes [10,16–21]. However, their dark current is generally larger than for III-V photodetectors due to defects of Ge formed during the processing. Furthermore, the absorption coefficient of Ge drops largely for wavelengths beyond 1550nm, inhibiting their applications for L band communication. As an alternative, it has been shown that high-quality III-V materials with large and wideband absorption coefficient can also be integrated on silicon by means of the aforementioned bonding process [11,12]. We have reported InGaAs PIN photodetectors integrated on Si with the help of a grating coupler [22] to diffract the light from SOI waveguides vertically to photodetectors so that a relatively thick bonding layer (~3 μ m) can be used [11]. However, like ordinary surface-illuminated detectors, there is a trade-off between the responsivity and the transition-time-limited bandwidth when choosing the thickness of the intrinsic InGaAs (i-InGaAs) absorption layer [23]. In this paper, instead, we adopt an evanescent coupling scheme to couple the light from the SOI waveguides to the InGaAs PIN photodetectors by using a very thin bonding layer (<200nm). Because of the phase matching between the SOI waveguide mode and the detector mode, the photodetector can use a thin absorption layer (100nm) and a short device length (40 μ m). The fabricated photodetectors show good performance in terms of dark current, responsivity, and wavelength range.

2. Design and fabrication

Figure 1 shows the schematic of the cross section of an InGaAs PIN photodetector integrated on an SOI waveguide. The size of the Si waveguide is 3 μ m \times 220nm. The III-V layer structure consists of an i-In_{0.53}Ga_{0.47}As layer sandwiched between a p-InP layer and an n-InP layer. All of the three layers are 100nm thick. The thickness of these three layers is optimized to achieve phase matching [24] between the SOI waveguide mode and the detector mode supported by these layers, so that an efficient evanescent coupling can be expected. And the coupling is not sensitive to the thickness of the BCB bonding layer as long as it is thin enough (<200nm), where a thinner bonding layer can be achieved by using a more diluted BCB solution. On top of the p-InP layer, there is a 50nm-thick, highly doped p-In_{0.53}Ga_{0.47}As layer in order to form a good ohmic contact with the p-metal sitting above. The whole p-contact layer stack (including the p-metal and p-InGaAs layers) is only present at the two sides of the SOI waveguide, in order to avoid detrimental optical absorption of the detector mode, which can be serious if the contact covers the whole detector mesa. The details of the device design can be found in Ref [25].

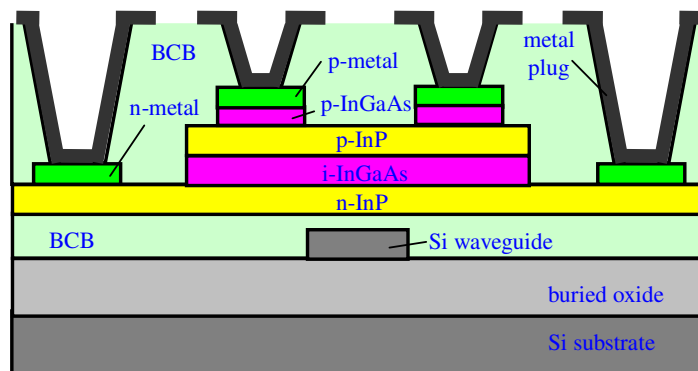


Fig. 1. The cross section of an InGaAs PIN photodetector integrated with an SOI waveguide.

The fabrication started with the DVS-BCB die-to-wafer bonding. After bonding the III-V die onto the patterned SOI substrate, the InP substrate was removed through a combination of mechanical grinding and chemical etching. Then a pair of InGaAs/InP sacrificial layers was removed by chemical wet etching, exposing the p-InGaAs contact layer. A Ti/Au p-metal contact was deposited. This metal pattern was lithographically aligned to the underlying SOI waveguide. Subsequently, the p-InGaAs layer was etched through by using this p-metal

contact layer as the etching mask. Then the detector mesa was defined by etching through the p-InP and i-InGaAs layers. The remaining n-InP layer was removed where it was not needed, e.g., on top of the access SOI waveguides and fiber grating couplers. The AuGe/Ni n-metal contact was then fabricated. A ~600nm-thick BCB dielectric layer was spin-coated on top of the whole device, and vias were opened (with an O₂ and SF₆ plasma etching process) down to the p- and n-metal contacts. Finally, another Ti/Au layer was deposited as the metal plugs as well as the probe pads. All the etching of the III-V materials was done with wet chemistry, in order to minimize the damage to the sidewalls. We used a solution of H₂SO₄:H₂O₂:H₂O (= 1:1:18) for InGaAs etching, and H₃PO₄:HCl (= 7:3) for InP etching. Both of the two solutions are highly selective to the non-targeted materials. Figure 2 shows the top view of a fabricated device before the final metallization for plugs and pads.

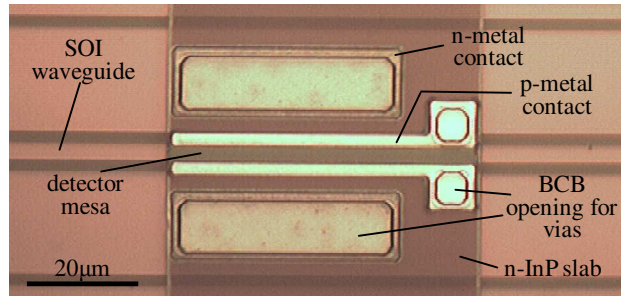


Fig. 2. Top view of a fabricated device before the final metallization for plugs and pads.

3. Measurement results

The length of the photodetectors under test was 40 μm. The current-voltage (I-V) characteristic was measured first. Figure 3 shows the I-V curve without light input. The measured dark current under zero and 0.5V bias is around 3pA and 10pA, respectively. Considering the minimal reliable current value of the measurement equipment (Keithley 2400) is 10pA, we can conclude that the dark current should be around (if no less than) 10pA. With higher reverse bias voltages, the dark current increases gradually but is still less than 150pA even at a reverse bias of 10V. This is several orders of magnitude lower than either Ge photodetectors reported in literature [10,16–21] or the AlGaInAs quantum-well photodetector [26] on silicon demonstrated previously. We attribute this low dark current level to the mild and noninvasive wet etching of the i-InGaAs layer and the timely passivation of the etched sidewalls. For the measurement of the photoresponse, TE-polarized light was coupled into the input SOI waveguides with the help of grating couplers [22]. The actual light power coupled into the photodetector was determined by measuring a reference SOI waveguide with the same grating couplers. Figure 4 shows the I-V curve under illumination at a wavelength of 1550nm. The input light power varies from 6.22nW to 62.2 μW in steps of 10dB. The internal responsivity is around 1.1A/W (corresponding to a quantum efficiency of 88%) and remains stable for a reverse bias ranging from 0V to 10V. Therefore, the proposed photodetector can work well even without an external bias. This measured high responsivity indicates an efficient evanescent coupling between the SOI waveguide and the III-V detector layers, a negligible detrimental absorption by the p-InGaAs and p-metal layers, and a sufficient light absorption for a 40 μm-long photodetector. The responsivity remains almost constant for a power range of 40dB, indicating a good linearity and dynamic range of the photoresponse. The low dark current of the present photodetector enables a reliable detection of the light power in the order of nW. Compared to our previously demonstrated InAlAs–InGaAs metal-semiconductor-metal (MSM) photodetectors integrated on SOI waveguides [27], the proposed InGaAs PIN photodetectors have a lower dark current due to the larger potential barrier formed by the PIN junction compared to that of the Schottky junction. The required bias voltage is also lower.

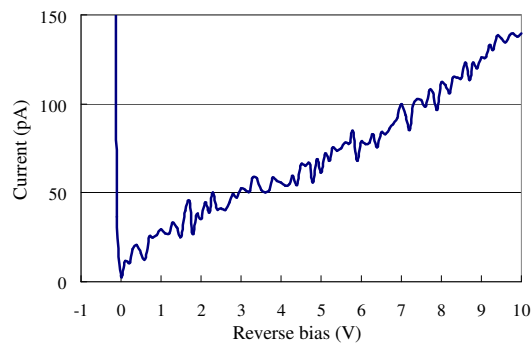


Fig. 3. I-V curve without light input.

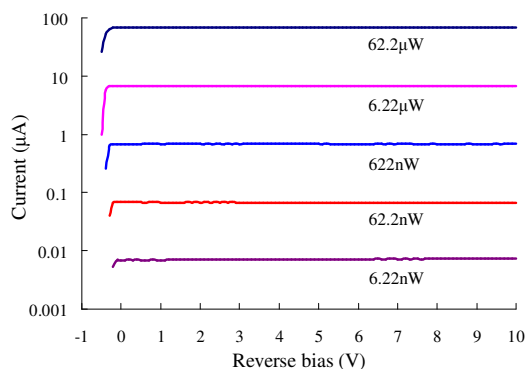


Fig. 4. I-V characteristics under illumination at a wavelength of 1550nm.

In order to evaluate the spectral response of the photodetector, the SOI chip was cleaved and a lensed fiber was used to couple light into the SOI waveguide. This overcomes the limited coupling bandwidth provided by the grating couplers. Figure 5 shows the normalized quantum efficiency (QE) as a function of wavelength. Due to the large absorption coefficient of InGaAs and the efficient evanescent coupling for a wide range of wavelength, the QE maintains over 90% of the peak efficiency up to 1580nm, and remains about 70% at the wavelength of 1640nm. The ripples in Fig. 5 may be due to the accidental environment fluctuation during measurement, not the device characteristics. Further measurement for shorter wavelengths was limited by the wavelength range of the tunable laser we used. However, InGaAs has even larger absorption coefficients for shorter wavelengths, and the simulation shows that the coupling between the detector mode and the SOI waveguide mode is still very efficient around a wavelength of 1310nm. Therefore, the photodetector can work for the whole S, C and L communication band, and can probably work well for even shorter wavelengths, e.g., the O-band. Further improvement of the responsivity for longer wavelengths can be achieved by using a thinner BCB bonding layer or a longer device length.

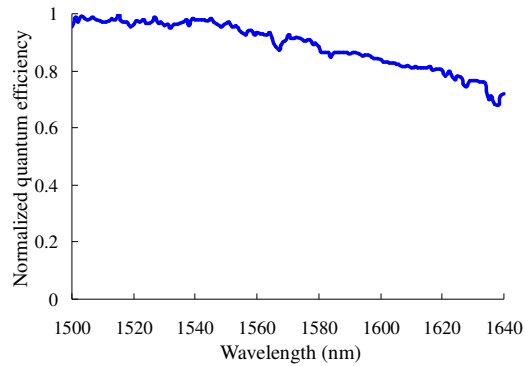


Fig. 5. Normalized quantum efficiency of the InGaAs photodetector.

For the current design, the electric field may be weak in the carrier-generated region since the p-contact layers only appear at the sides of the photodetector. This can influence the transit time of the carriers to the contacts. Therefore, a large bias voltage may be required for high-speed applications. High-speed measurement will be conducted to investigate this issue in the future.

4. Conclusion

High performance InGaAs PIN photodetectors integrated on SOI waveguides were fabricated and characterized. With proper design of the device structure, efficient evanescent coupling between SOI waveguides and InGaAs photodetectors was achieved. The fabricated photodetector has a very low dark current of 10pA and a high responsivity of 1.1A/W. It can also work for a wide wavelength range covering the whole S, C, and L communication band. The photodetectors can be easily integrated with various functional passive SOI devices. For example, they can be integrated with an arrayed waveguide grating (AWG) demultiplexer [28] to form a wavelength division multiplexing (WDM) receiver.

Acknowledgements

The authors would like to thank S. Verstuyft and Z. Yu for processing assistance. Z. Sheng acknowledges the China Scholarship Council for a student grant. This work is partially supported by the EU project ICT-BOOM under the 7th Framework Programme.